nature plants

ARTICLES

PUBLISHED: XX XX 2014 | ARTICLE NUMBER: 15176 | DOI: 10.1038/NPLANTS.2015.176

# An intact light harvesting complex I antenna system is required for complete state transitions in *Arabidopsis*

Samuel L. Benson[1†], Pratheesh Maheswaran[2†], Maxwell A. Ware[2], C. Neil Hunter[1], Peter Horton[1], Stefan Jansson[3], Alexander V. Ruban[2] and Matthew P. Johnson[1*]

**Efficient photosynthesis depends on maintaining a balance between the rate of light-driven electron transport occurring in the reaction centres of the two photosystems (PSI and PSII) located in the chloroplast thylakoid membranes. Balance is achieved through a process of 'state transitions' that increases energy transfer towards PSI when PSII is overexcited (State II), and towards PSII when PSI is overexcited (State I). This is achieved through redox control of the phosphorylation state of light-harvesting antenna complex II (LHCII). PSI is served by both LHCII and four light-harvesting antenna complex I (LHCI) subunits, Lhca1, 2, 3 and 4. Here we demonstrate that despite unchanged levels of LHCII phosphorylation, absence of specific Lhca subunits reduces state transitions in *Arabidopsis*. The severest phenotype—observed in a mutant lacking Lhca4 (ΔLhca4)—has a 69% reduction compared with the wild type. The amounts of the PSI–LHCI–LHCII supercomplex isolated by blue native polyacrylamide gel electrophoresis (BN-PAGE) from digitonin-solubilized thylakoids were similar in the wild type and ΔLhca mutants. Fluorescence excitation spectroscopy revealed that in the wild type this PSI–LHCI–LHCII supercomplex is supplemented by energy transfer from additional LHCII trimers in State II, whose binding is sensitive to digitonin, and which are absent in ΔLhca4. The grana margins of the thylakoid membrane were found to be the primary site of interaction between this 'extra' LHCII and the PSI–LHCI–LHCII supercomplex in State II. The results suggest that the LHCI complexes mediate energetic interactions between 'extra' LHCII and PSI in the intact membrane.**

Plants regulate the light-harvesting antenna size of PSI and PSII to balance the rate of photochemistry of each reaction centre and so optimize photosynthetic electron transport in response to light quantity and spectral quality[1,2]. Known as state transitions, this mechanism is controlled by the redox state of the intersystem electron carrier plastoquinone (PQ)[3]. When the PQ pool is reduced the membrane-associated STN7 serine-threonine kinase begins to phosphorylate the Lhcb1 and Lhcb2 subunits of the major trimeric LHCII (ref. 4). Phosphorylation of LHCII leads to its dissociation from PSII and association with PSI (State II), rebalancing the input of excitation energy between the photosystems over several minutes. When the PQ pool becomes oxidized the STN7 kinase is deactivated and the constitutively active TAP38/PPH1 phosphatase dephosphorylates LHCII leading to its re-association with PSII (State I)[5,6]. The absence of state transitions in ΔSTN7 *Arabidopsis* significantly reduces their growth rate under fluctuating light conditions, highlighting the importance of this regulatory mechanism for plant fitness[7,8].

PSII and PSI are segregated in thylakoid membranes, with the former residing mainly in the stacked grana regions and the latter in the unstacked stromal lamellae and grana margin regions[9]. LHCII binds to PSII at three sites named S (strong), M (medium) and L (loose)[10]. PSII assembles *in vivo* as a dimer binding two copies each of the M and S trimers, forming the $C_2S_2M_2$ supercomplex[10]. The S trimer is formed from Lhcb1 and 2 subunits, while the M trimer comprises Lhcb1 and Lhcb3[11]. Since the structure of the PSII–LHCII supercomplex is unchanged following phosphorylation[12] and given PSI binds no Lhcb3 in State II (ref. 11), the S and M trimers are unlikely to be involved in state transitions. Therefore, the peripherally bound 'L' trimers were suggested to interact with PSI in State II (ref. 11). Electron microscopy has shown that LHCII phosphorylation leads to a partial reduction in the number of layers and lateral dimensions of the grana stacks[13–15]. The changes in membrane structure result in enrichment of LHCII in the stromal lamellae, and PSI in the grana margins, facilitating increased contact between the two complexes in State II[13,16,17]. A PSI–LHCII supercomplex is formed in State II, which depends on the presence of the PsaL and PsaH subunits of PSI that form the docking site for LHCII[11,18–20].

On the opposite side of the PSI complex from the PsaH/L binding site of LHCII and not believed to be involved in state transitions are the four LHCI subunits, Lhca1, 2, 3 and 4 (refs. 21–23). Each Lhca subunit shows a 1:1 stoichiometry with PSI, forming a PSI–LHCI supercomplex[24–26]. Lhca1 and 4 form a dimeric LHCI complex closest to the PsaG subunit, while Lhca2 and 3 form a second dimer binding closest to PsaK (ref. 26). Absence of Lhca2 or 4 also resulted in a strong reduction of the amount of their dimeric partners, in both the PSI–LHCI supercomplex[26] and thylakoids[24,27–30]. In contrast, loss of Lhca1 or Lhca3 did not destabilize Lhca2 and 4 binding to the same extent[26]. In the following study we investigated how loss

[1]Department of Molecular Biology and Biotechnology, University of Sheffield, Firth Court, Western Bank, Sheffield S10 2TN, UK. [2]School of Biological and Chemical Sciences, Queen Mary University of London, Mile End Road, London E1 4NS, UK. [3]Department of Plant Physiology, Umeå Plant Science Centre, Umeå University, Umeå SE-901 87, Sweden. †Present addresses: Rothamsted Research, West Common, Harpenden, Hertfordshire AL5 2JQ, UK (S.L.B.); Allied Health Sciences Unit, Faculty of Medicine, University of Jaffna, Aadiyapatham Road, Kokuvil East, Kokuvil, Sri Lanka (P.M.).
*e-mail: matt.johnson@sheffield.ac.uk

of the Lhca 1, 2, 3 and 4 subunits affects state transitions in *Arabidopsis*. The results demonstrate an unexpected role for LHCI in energetically connecting LHCII to PSI in State II.

## Results

**Loss of Lhca subunits impairs state transitions.** State transitions can be measured by pulse amplitude modulated (PAM) chlorophyll fluorescence, using red (635 nm) and far-red (720 nm) light to preferentially excite PSII and PSI respectively[1,2]. Figure 1 compares fluorescence traces for the wild type and mutants (ΔLhca1, ΔLhca2, ΔLhca3 and ΔLhca4). The first part of the trace in which plants were illuminated with both red and far-red light shows the transients associated with the activation of electron transport and the Calvin cycle. After 5 min the far-red light is switched off causing a rapid rise in the fluorescence level (*F*s). The *F*s rise results from less efficient quenching of the PSII antenna by photochemistry due to over-reduction of the PQ pool. Throughout the subsequent 20 min in the wild type, *F*s gradually returns to a value similar but not identical to that seen before the far-red light was switched-off (Fig. 1a). The fall in Fs is related to the state transition, which increases the photochemical rate of PSI, thus re-oxidizing the PQ pool. A saturating light pulse is then applied to determine *F*m′II (the maximum level of fluorescence in State II). Following this cycle the far-red light is reapplied, and *F*s rises gradually over 20 min as LHCII is dephosphorylated and reconnected to PSII. A second saturating pulse is then applied to determine Fm′I. The mutants displayed a larger rise in *F*s upon removal of far-red light and a slower and less complete state transition (Fig. 1b–f). The severest state transition phenotype (measured by the qT method) is seen in ΔLhca4, which has just 31% of the wild-type level, compared with around 52–63% in ΔLhca1, 2 and 3 (Table 1). Consistent with the disruption to state transitions, an increased reduction of the PQ pool is also observed in the mutants (Table 1).

**Absence of Lhca subunits does not affect LHCII phosphorylation.** We tested the phosphorylation state of the thylakoid proteins in State I or State II light conditions using the Diamond Pro-Q Phospho stain. Both the wild type and mutants showed increased phosphorylation of LHCII and the PSII core subunits D1, D2 and CP43 in State II (Fig. 1g). However, there was no significant difference in the level of LHCII phosphorylation between the wild type and mutants in either State I or II (Fig. 1g and Supplementary Fig. 1a). Similar results were obtained by anti-phosphothreonine antibody immunoblotting (Supplementary Fig. 1b). These results imply that the deficiency in state transitions is not due to altered activity of the STN7 kinase or PPH1/TAP38 phosphatase.

**Loss of Lhca subunits impairs energy transfer from LHCII to PSI.** The antenna size of PSI in the wild type and mutants was determined by measuring the photo-oxidation kinetics of the PSI reaction centre (P700) using absorption spectroscopy (Fig. 2a,b). Fitting the curves with monoexponential functions showed the PSI antenna size in State I was 84, 72, 82 and 55% of the wild type in ΔLhca1, 2, 3 and 4 respectively (Fig. 2a and Table 2). In State II we calculated an increase of 28% in PSI antenna size in the wild type, consistent with the 25–33% increase previously reported[2,18] (Fig. 2b and Table 2). If state transitions were unperturbed in the mutants, a larger percentage increase in antenna size in State II would be predicted, given their smaller antenna size in State I. In contrast, the PSI antenna size in ΔLhca1, 2, 3 and 4 was increased only by 19, 17, 16 and 17% relative to the State I situation in each sample. The $P700^+$ absorption data therefore shows that the absolute amount of LHCII energetically coupled to PSI in State II is reduced.

We also quantified PSI antenna size by low temperature (77 K) fluorescence emission and excitation spectroscopy. In the wild-type thylakoids the fluorescence emission showed a large increase in the ratio of the 730 nm PSI band compared to the 685 nm PSII band (Fig. 2c). The PSI emission in ΔLhca1, 2, 3 and 4 thylakoids was blue-shifted from 730 nm in the wild type to 728, 724, 725 and 722 nm respectively ΔLhca1, 2, 3 and 4 (Fig. 2c)[27–30]. The increase in the intensity of the PSI band relative to the 685 nm PSII band in State II was also much smaller in the mutants (Fig. 2c). The increase in PSI antenna size due to state transitions can be calculated by comparing the excitation spectra for 735 nm emission, where PSI contribution is dominant. The spectra are normalized at 705 nm, the PSI–LHCI terminal emitter region, where there is no absorption by PSII or LHCII (refs 2,20) (Fig. 2d). A 32% increase in PSI antenna size, expressed as the ratio between the difference spectrum and State I spectrum, was calculated for the wild type. The PSI excitation spectra of the mutants showed differences with the wild type, consistent with the selective loss of specific Lhca subunits in each case[24] (Fig. 2d). PSI antenna size increased in State II by 18, 16, 21 and 23% in ΔLhca1, 2, 3 and 4, respectively, confirming the $P700^+$ measurements that show the change is smaller than in the wild type. Nonetheless, the spectral shape of the State II-*minus*-State I difference spectrum in each case still closely resembled that of the purified LHCII trimer, confirming that some association between PSI and LHCII still exists in State II in these mutants (Supplementary Fig. 2a). The changes in PSII antenna size during state transitions were also checked by monitoring the excitation spectra for 705 nm emission, where PSII dominates (Supplementary Fig. 2b). In the wild type the PSII antenna size decreased by 13% in State II, whereas smaller decreases of 9, 8, 8 and 4% were recorded in ΔLhca1, 2, 3 and 4, respectively. Therefore, in the mutants a larger proportion of the LHCII antenna remains energetically coupled to PSII under State II conditions.

To assess the relative difference in PSI and PSII antenna size, the area under the 705 and 735 nm excitation spectra recorded for State II were normalized to the 685–735 nm emission ratio and then subtracted to give PSII-*minus*-PSI difference spectra (Fig. 2e). ΔLhca4 shows the greatest difference between PSI and PSII in the absorption of light at 620–670 nm, consistent with the smaller PSI antenna size in this mutant (Fig. 2e). The relative absorption by PSI of far-red light was also weakest in ΔLhca4, consistent with the loss of some of the far-red absorbing chlorophylls in this mutant[24] (Fig. 2e). When the absorption difference at 635 nm (State II light) is plotted against the 1-qP value of each mutant in State II (Table 1), a negative linear correlation is observed (Fig. 2f). Therefore the larger differences in the absorption of red light by PSII and PSI results in an increased imbalance in their electron transfer rates and thus increased reduction of the PQ pool in the mutants.

**Effect of Lhca on PSI–LHC supercomplex formation.** Previous studies of thylakoid membranes solubilized with the detergent digitonin demonstrated formation of a supercomplex comprising PSI–LHCI and one LHCII trimer in State II (refs. 11,20). We analyzed thylakoids prepared in State I or State II from the wild type and mutants (Fig. 3a), using a similar protocol of digitonin solubilization and fractionation using BN–PAGE[31]. Several bands are resolved in the BN–PAGE gel (Fig. 3a), whose identities were confirmed by denaturing PAGE in the second dimension (Supplementary Fig. 3a) as (from top of the gel to bottom) (1) PSI–LHCI–LHCII supercomplex, (2) PSI–LHCI, (3) ATP synthase, (4) PSI core, (5) PSII core, (6) cytochrome $b_6f$ (cyt$b_6f$) and (7) trimeric LHCII. The enrichment in PSI-associated bands relative to PSII in the digitonin solubilized material reflects the composition of the stromal lamellae and grana margins that are accessible to this detergent, while the PSII-enriched grana membranes remain largely unsolubilized[31]. Consistent with

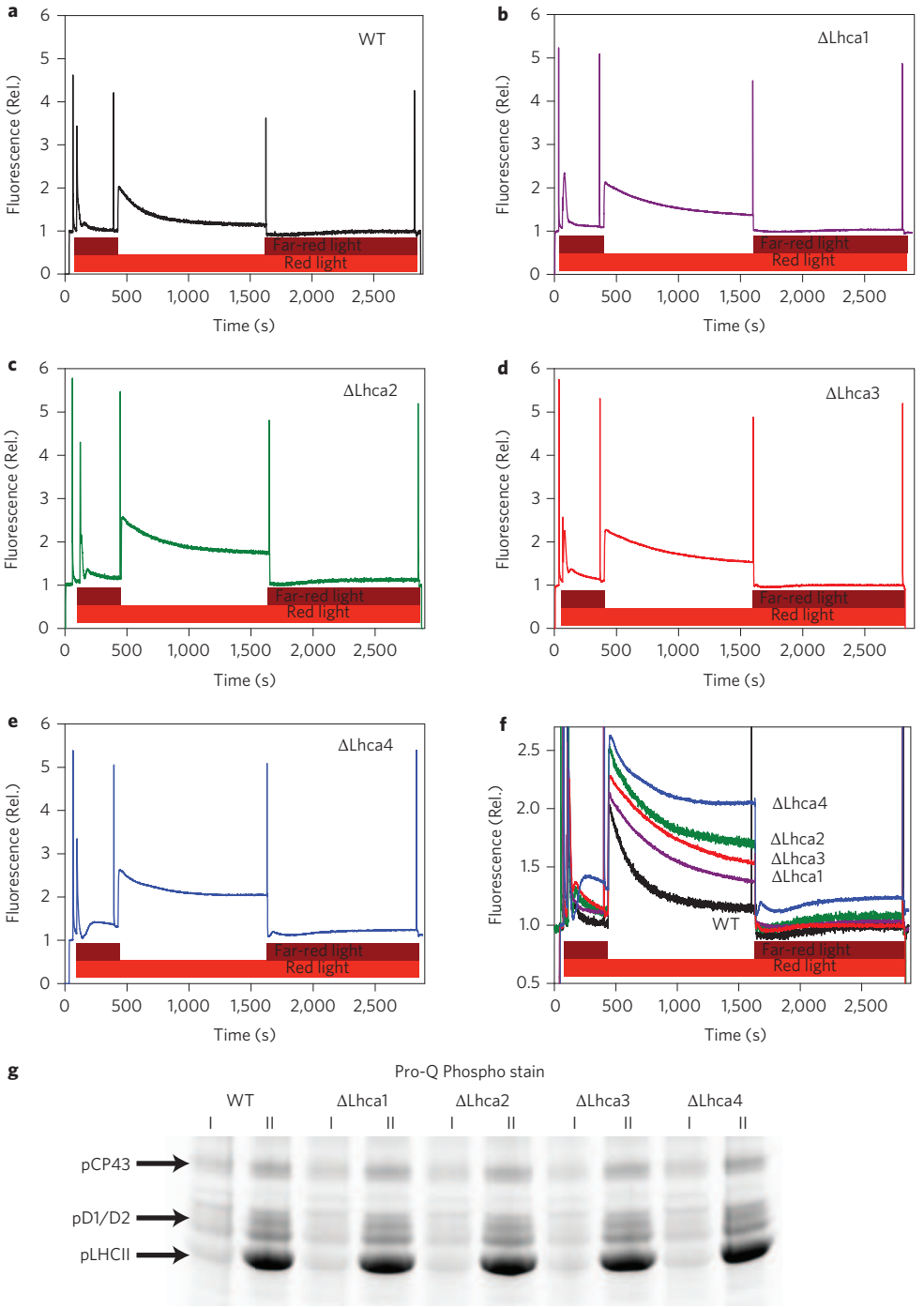


**Figure 1 | State transitions and thylakoid protein phosphorylation in wild-type and ΔLhca plants. a–e,** PAM fluorescence traces showing state transitions in wild type (**a**), ΔLhca1 (**b**), ΔLhca2 (**c**), ΔLhca3 (**d**) and ΔLhca4 (**e**) plants. **f**, Comparison of state transition kinetics, colours as in **a–e**. All traces are normalized to unity at Fo. **g**, Pro-Q Phospho stained SDS-PAGE gel of total thylakoid proteins from wild-type and ΔLhca mutants.

expectations, in the wild-type State II sample a prominent band belonging to the PSI–LHCI–LHCII supercomplex appears above the PSI–LHCI band that is absent in State I (Fig. 4a).

In State I ΔLhca1 and 3, band 2 migrates slightly further (Fig. 3a), as expected for a PSI–LHCI complex lacking these specific Lhca subunits[26]. A small amount of PSI cores lacking any Lhca subunits (band 4) (Fig. 3a and Supplementary Fig. 3b,c) are also observed in ΔLhca1 and 3, despite being virtually absent in the wild type. Upon transition to State II a new band (band 1) appears ΔLhca1 and 3 above the PSI–LHCI band that is a PSI–LHCI–LHCII supercomplex lacking the respective Lhca subunit in each case (Fig. 3a and Supplementary 3b,c). The situation in ΔLhca2 differs slightly. Firstly, an additional band 2 is observed in State I (labelled band 2b in Fig. 3a) that is the smaller PSI–LHCI complex lacking both Lhca2 and 3, as previously described[26] (Fig. 3a and Supplementary Fig. 3d). In State II band 1 appears but migrates faster than in the wild type and corresponds to a PSI–LHCI–LHCII supercomplex lacking Lhca2 (Fig. 3a and Supplementary Fig. 3d). In ΔLhca4, band 2 is virtually absent but band 2b, representing a PSI–LHCI complex lacking Lhca1 and 4, is present alongside a much larger amount of 'free' PSI core complex lacking all Lhca subunits[25,26] (Fig. 3a and Supplementary Fig. 3e). Upon transition

**Table 1 | Fluorescence parameters of wild-type and ΔLhca mutant plants.**

| Sample | *Fv/Fm* | | qS | qS ($t_{½}$, s) | 1-qP |
|---|---|---|---|---|---|
| Wild type | 0.79 ± 0.02 | 0.121 ± 0.01 | 0.81 ± 0.06 | 144 ± 11 | 0.074 ± 0.01 |
| ΔLhca1 | 0.82 ± 0.02 | 0.076 ± 0.02 | 0.69 ± 0.05 | 229 ± 22 | 0.0970 ± 0.05 |
| ΔLhca2 | 0.83 ± 0.01 | 0.064 ± 0.01 | 0.62 ± 0.05 | 275 ± 33 | 0.17 ± 0.07 |
| ΔLhca3 | 0.83 ± 0.01 | 0.074 ± 0.02 | 0.66 ± 0.07 | 245 ± 27 | 0.12 ± 0.04 |
| ΔLhca4 | 0.82 ± 0.01 | 0.038 ± 0.01 | 0.33 ± 0.05 | 230 ± 25 | 0.243 ± 0.07 |

*Fv/Fm*, is the maximum quantum yield of PSII in the dark prior to illumination, qT and qS are measures of state transitions, qT is the fluorescence decline associated with movement of LHCII from PSII to PSI and qS measures how effectively state transitions are at rebalancing electron transport[2], qS ($t_{½}$) is the half-time taken to reach 50% of the total qS, 1-qP is a measure of the redox state of the intersystem electron carrier plastoquinone in State II.

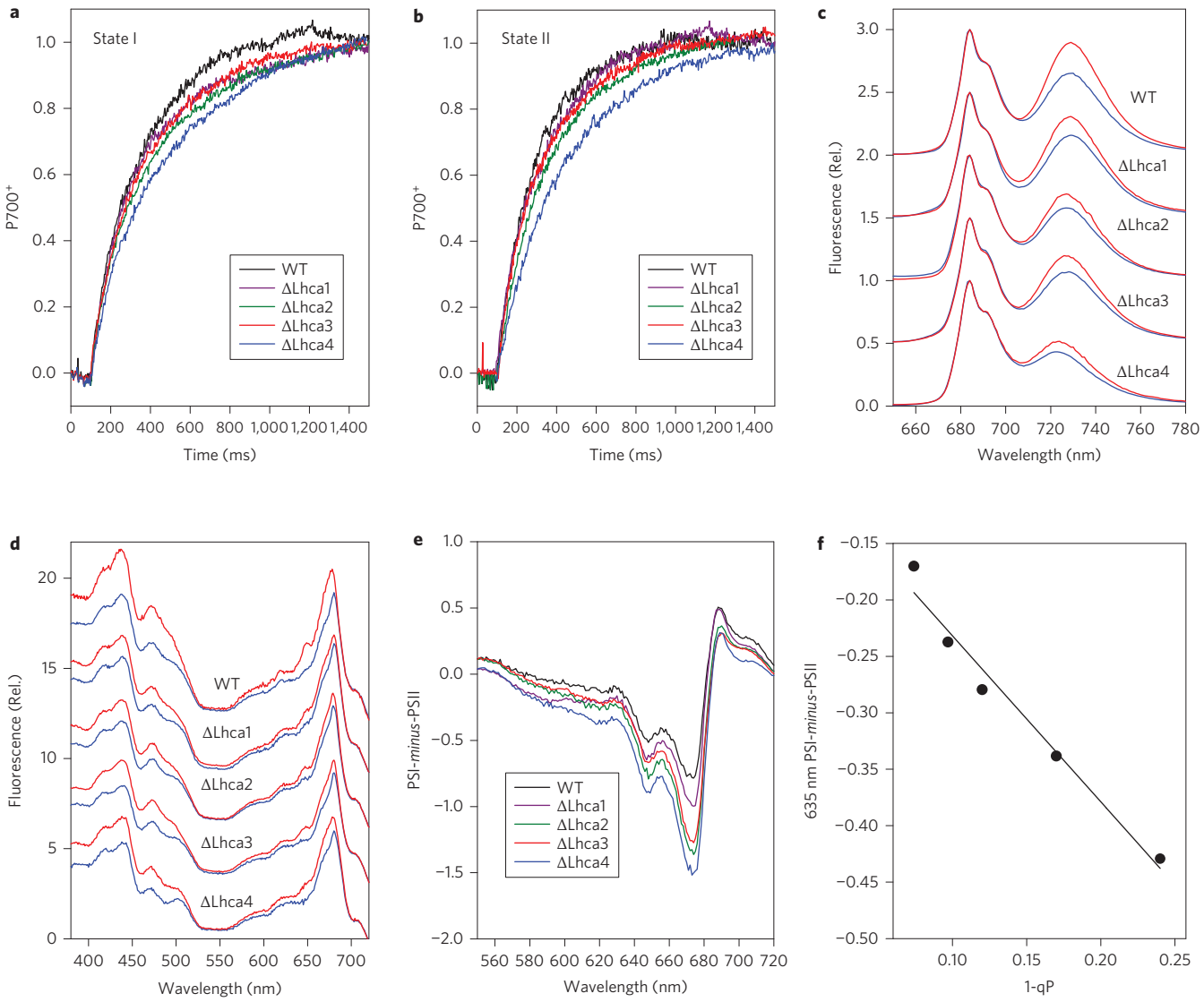


**Figure 2 | Determination of PSI antenna size in wild-type and ΔLhca plants. a**,**b**, P700$^+$ formation kinetics (830–875 nm) measured by absorption spectroscopy on wild-type (black trace), ΔLhca1 (purple), ΔLhca2 (green), ΔLhca3 (red) and ΔLhca4 (blue) thylakoids in State I (**a**) and State II (**b**). **c**, Low temperature (77 K) fluorescence emission spectra (435 nm excitation, spectra were normalized at 685 nm). **d**, PSI low temperature (77 K) fluorescence excitation spectra (735 nm emission, spectra were normalized at 705 nm). State I is shown in blue, State II in red. **e**, PSI-*minus*-PSII excitation difference spectra as labelled, the area underneath the spectra were scaled according to the 685/735 nm emission ratio. **f**, Relationship between the PSI and PSII excitation spectra difference at 635 nm in State II and the 1-qP value measured after 20 min of acclimation to red light (Table 1).

to State II, band 1 appears in ΔLhca4, but migrating faster than in the wild type, representing a PSI–LHCI–LHCII supercomplex lacking Lhca1 and 4 (Fig. 3a and Supplementary 3e). Band 2b also increases at the expense of band 4 and this band now contains LHCII, suggesting formation of a PSI core–LHCII supercomplex lacking any Lhca proteins (Fig. 3a and Supplementary Fig. 3e). Densitometric analysis of the PsaA/B PSI core subunit spot in Sypro-stained 2D gels indicates that 43, 39, 42, 41 and 50% of PSI is present in bands also containing LHCII in the wild type and ΔLhca1, 2, 3 and 4 respectively (Fig. 3b). The biochemical analysis therefore shows that despite the strong reduction in state transitions in the mutants, the amount of PSI complexes binding LHCII, as

**Table 2 | PSI functional antenna size in wild-type and ΔLhca mutant thylakoids determined by absorption spectroscopy.**

| Sample | State IP700$^+$ ($t_{½}$, ms) | State IIP700$^+$ ($t_{½}$, ms) | Calculated PSI antenna size % of wild type in State I | | % increase in PSI antenna size in State II |
|---|---|---|---|---|---|
| | | | State I | State II | |
| Wild type | 179 ± 5 | 140 ± 8 | 100% | 128 ± 3% | 28 ± 3% |
| ΔLhca1 | 210 ± 6 | 174 ± 6 | 84 ± 3% | 96 ± 3% | 19 ± 4% |
| ΔLhca2 | 241 ± 5 | 212 ± 10 | 74 ± 3% | 84 ± 5% | 16 ± 4% |
| ΔLhca3 | 217 ± 9 | 185 ± 8 | 82 ± 5 | 96 ± 3% | 17 ± 4% |
| ΔLhca4 | 324 ± 9 | 278 ± 11 | 55 ± 5% | 64 ± 6% | 17 ± 3% |

P700$^+$ formation kinetics (830–875 nm) were measured on isolated thylakoid membranes presence of 30 μM DCMU, 100 μM methyl viologen and 500 μM sodium ascorbate to create a donor-limited situation. Traces were fitted with a single exponential functions and the tabulated data is the average of four traces per sample. The light intensity was 29 μmol photons $m^{-2}$ $s^{-1}$. PSI antenna size is calculated as (wild-type State I $t_{½}$ ÷ sample $t_{½}$) × 100% expressed as a percentage of wild-type State I.

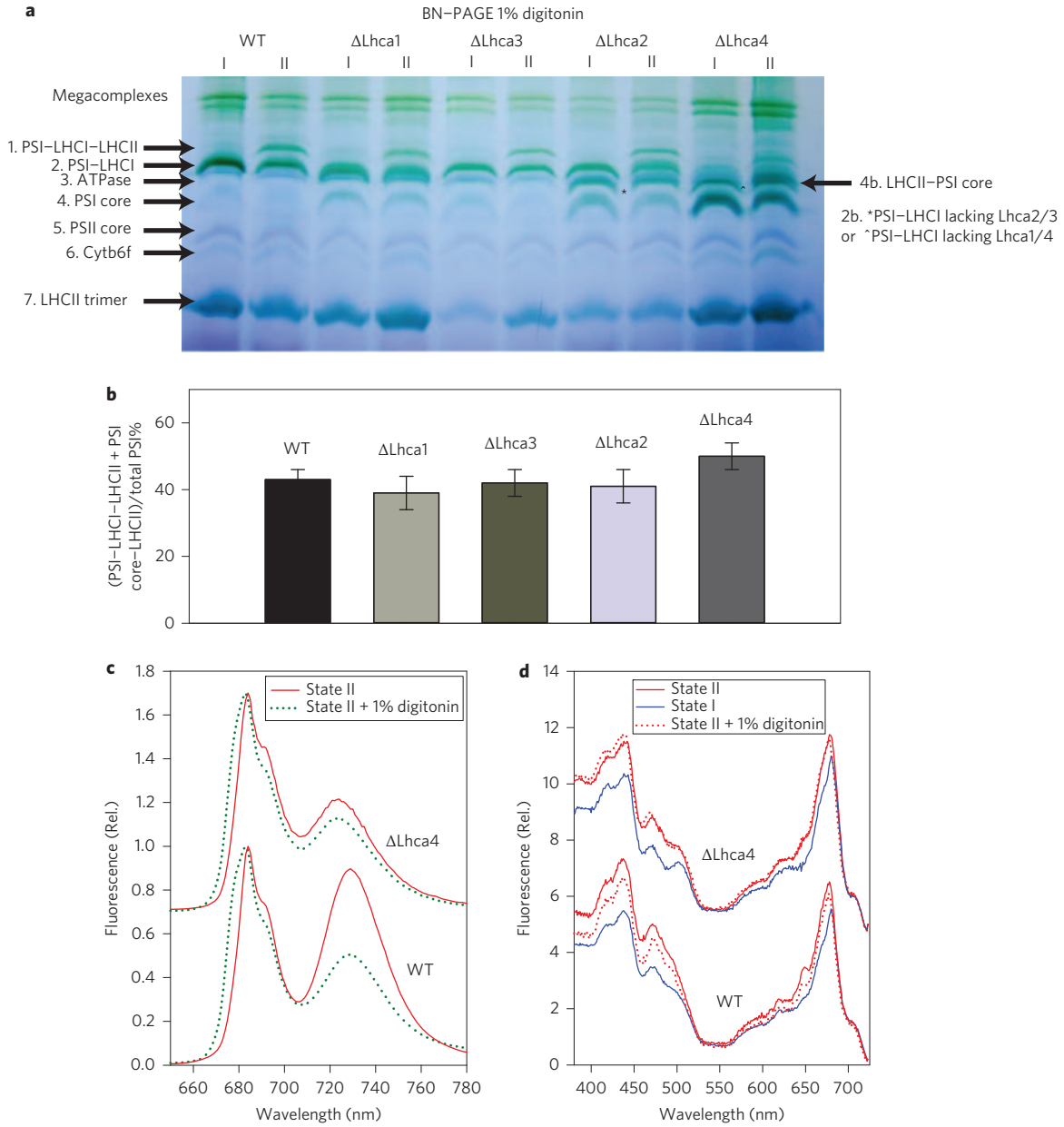


**Figure 3 | Effect of digitonin on PSI–LHCII interaction in wild-type and ΔLhca thylakoids. a**, BN–PAGE of supernatant from 1% digitonin solubilization of thylakoid membranes from wild type and ΔLhca mutants. **b**, Relative amounts of PSI binding LHCII as derived from scanning of the PsaA/B PSI core subunits spot in Sypro-stained 2D gels in Supplementary Fig. 3. **c**,**d**, Low temperature (77 K) fluorescence emission spectra (435 nm excitation, spectra were normalized at 685 nm) (**c**) and PSI low temperature (77 K) fluorescence excitation spectra (735 nm emission spectra were normalized at 705 nm) (**d**) following 1% digitonin treatment of State II thylakoids (dashed line) compared to untreated State I (solid blue line) and State II (solid red line) wild-type and ΔLhca4 thylakoids.

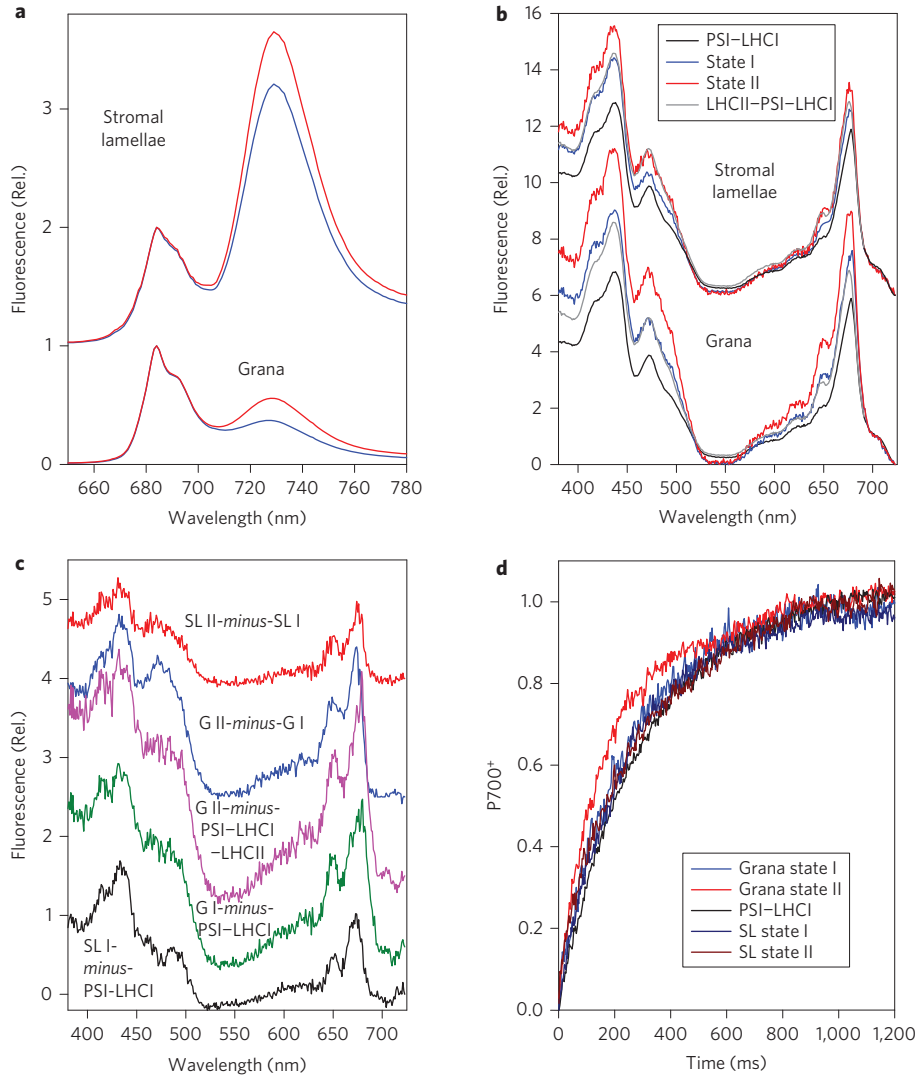


**Figure 4 | PSI antenna size in wild-type grana and stromal lamellae membranes. a**,**b**, Low temperature (77 K) fluorescence emission spectra (435 nm excitation, spectra were normalized at 685 nm) (**a**) and PSI low temperature (77 K) fluorescence excitation spectra (735 nm emission spectra were normalized at 705 nm) (**b**) of isolated wild-type State I (blue) and State II (red) grana and stromal lamellae compared to isolated PSI–LHCI (black) and PSI–LHCI–LHCII (grey) supercomplexes. **c**, State I-*minus*-State II excitation difference spectrum for grana (G) and stromal lamellae (SL) and relative differences compared to purified PSI–LHCI. **d**, $P700^+$ formation kinetics (830–875 nm) measured by absorption spectroscopy on isolated grana and stromal lamellae.

determined by the Digitonin BN–PAGE method, is similar to the wild type.

We next analyzed whether the increase in PSI antenna size in State II, determined by excitation fluorescence and absorption spectroscopy, could be explained by the amount of PSI binding LHCII observed by the Digitonin BN–PAGE method. Assuming that the in wild-type State I corresponds to the antenna size in the PSI–LHCI complex (155 chlorophylls)[22,23], then 55% of this is ~85 chlorophylls for ΔLhca4. If 50% of this binds 42 extra chlorophylls (one LHCII trimer)[32] then the increase would be 25%, consistent with the 23% rise observed (Fig. 2d). In contrast, the 32% rise observed in wild-type PSI antenna size in State II would imply an extra ~1.2 trimers are bound per PSI. Clearly this is not observed by the Digitonin BN–PAGE method where only ~45% of PSI can be isolated with LHCII bound (Fig. 3b). Therefore a clear discrepancy emerges between the two sets of data.

**Lhca proteins mediate energy transfer between the "extra" LHCII and PSI.** Recent evidence implies that energy transfer from LHCII to PSI is disrupted by the addition of digitonin to thylakoid membranes[33]. These data suggested that the stable PSI–LHCI–LHCII supercomplex isolated by the Digitonin BN–PAGE method from State II thylakoids may be supplemented by energy transfer from extra LHCII trimers, whose binding is more sensitive to the presence of digitonin. Indeed, large proportions of 'free' LHCII trimers are recovered upon even gentle solubilization of thylakoids with digitonin (see Fig. 3a, band 7). To investigate this further, we followed the approach of Grieco *et al.*[33] adding 1% digitonin to the State II wild-type and ΔLhca4 thylakoids and assessing the changes in the 77 K thylakoid fluorescence emission spectrum (Fig. 3c). The total fluorescence emitted by the PSII bands was increased relative to PSI in the presence of digitonin, with a strong shoulder appearing at ~680 nm that is characteristic for emission from uncoupled LHCII trimers (Fig. 3c). The relative decrease in the PSI emission band in the ΔLhca4 mutant was clearly smaller than that seen for the wild type. The result could imply that more LHCII is energetically disconnected from PSI in the wild type than in ΔLhca4 by the digitonin treatment. To check this we compared the PSI 77 K fluorescence excitation spectra for the digitonin-treated wild-type and ΔLhca4 thylakoids

to those obtained on intact thylakoids (Fig. 3d). The results show that the PSI antenna size is decreased by the digitonin treatment by ~50–60% in the wild type, but no clear decrease could be seen in ΔLhca4 (Fig. 3d). Therefore in the wild type there is a population of LHCII transferring energy to PSI in State II, whose connectivity is sensitive to digitonin and is absent in ΔLhca4.

**'Extra' LHCII interacts with PSI in the grana margins.** To investigate the membrane location of the 'extra' digitonin-sensitive fraction of LHCII bound to PSI, we fractionated the wild-type digitonin-solubilized thylakoids by differential centrifugation to obtain grana and stromal lamellae (Supplementary Table 1). These membrane fractions were then analyzed by 77 K fluorescence emission and excitation spectroscopy (Fig. 4a,b). The PSII bands at 685 and 693 nm dominate the emission spectrum of the grana with a smaller peak at 730 nm, belonging to PSI located in the grana margins (Fig. 4a). The intensity of the 730 nm PSI band in the grana fraction increases upon transition to State II (Fig. 4a). When the excitation spectra for 735 nm PSI emission in the State I and State II grana fractions are compared, a 37% increase in PSI antenna size is observed in State II, slightly larger than the 32% change averaged across the whole thylakoid (Fig. 2d). The emission spectrum of the stromal lamellae is dominated by the PSI band at 732 nm, which increases in intensity slightly in State II relative to the 685 nm PSII band (Fig. 4a). The 735 nm PSI excitation spectra of the stromal lamellae show a smaller 14% increase in PSI antenna size in State II (Fig. 4b). The shape of the State II-*minus*-State I excitation difference spectra for grana and stromal lamellae is consistent with trimeric LHCII (Fig. 4c). We compared the excitation spectra of purified wild-type PSI–LHCI and PSI–LHCI–LHCII complexes to those obtained for the grana and stromal lamellae (Fig. 4b). The PSI antenna size was similar in the isolated PSI–LHCI–LHCII supercomplex and State II stromal lamellae, but was larger in the grana (Fig. 4b). The State II grana-*minus*-PSI–LHCI–LHCII supercomplex difference spectrum demonstrated that this was due to binding of 'extra' LHCII (Fig. 4c). Surprisingly, in State I the PSI antenna sizes in stromal lamellae and grana were both larger than that of the isolated PSI–LHCI complex (Fig. 4b). In the case of the State I grana, the spectrum more closely resembled that of the PSI–LHCI–LHCII supercomplex (Fig. 4b). Again, the excitation difference spectra showed features consistent with LHCII, though they were slightly red-shifted, which may be due to the slight blue-shift of the Qy maximum in the purified PSI–LHCI complex (Fig. 4c). The excitation data therefore suggest that PSI in the grana margins receives more than 1 LHCII trimer per PSI as described by the current model of state transitions[1]. Moreover, it seems that some LHCII still transfers energy to PSI in the virtual absence of LHCII phosphorylation. Finally, we checked the PSI antenna size in the grana and stromal lamellae compared to purified PSI–LHCI by $P700^+$ absorption spectroscopy (Fig. 4d). The PSI antenna size was found to be 116% and 157% in States I and II in the grana and 107% and 116% in the stromal lamellae compared with the purified PSI–LHCI complex (Supplementary Table 1), confirming the conclusions drawn from the excitation spectroscopy.

## Discussion

In this work we uncovered an unexpected role for the LHCI antenna system in energetically connecting LHCII to PSI. The mutants showed a clear reduction in the amount of state transitions compared with the wild type, with the largest decrease seen in ΔLhca4. The state transitions phenotype may explain the strongly reduced Darwinian fitness of ΔLhca mutants, particularly ΔLhca4, observed in field experiments[29]. We note the absence of the PsaG, and PsaK PSI core subunits, which bind on the LHCI side of the PSI–LHCI, have previously been found to decrease state transitions by around ~30%[34,35]. The levels of PsaG and PsaK are the same as wild type in the mutants[26], while the levels of Lhca subunits are somewhat reduced in the absence of PsaG and PsaK (refs 34,35). As such, we can conclude the reduced state transition phenotype in these mutants is caused by the absence of Lhca subunits. It is noteworthy that the absence of PsaH or PsaL reduces state transitions by ~60–70%[18], suggesting that some LHCII is still able to transfer energy to PSI via another route in these mutants. In light of our results, it appears that this alternative pathway involves the Lhca subunits.

We found the PSI antenna size in the mutants was reduced in both State I and State II compared with the wild type. Impairment of state transitions meant larger differences in the efficiency of red light (620–670 nm) absorption by PSI and PSII exist in the mutants, particularly in State II. The result is an increase in the reduction of the PQ pool in the mutants under red light illumination, indicative of a greater imbalance in photochemical rate between the photosystems. Despite the state transition phenotype we found that the levels of LHCII and PSII phosphorylation were unperturbed in these mutants. In addition, the PSI–LHCI–LHCII supercomplex could still be isolated in similar yields from the mutants and the wild type, ~40–50% of the total solubilized PSI. This result led us to investigate the extent to which the PSI antenna size *in vivo* detected by absorption and excitation fluorescence spectroscopy matched the amount of PSI–LHCI–LHCII supercomplex isolated by the Digitonin BN–PAGE method. Intriguingly, the amount of PSI binding LHCII in ΔLhca4 matched the *in vivo* changes in antenna size, while in the wild type it did not. We thus investigated whether solubilization with 1% digitonin would affect the PSI antenna size measured by fluorescence excitation spectroscopy. In the wild type the PSI antenna size was reduced by ~50–60% due the digitonin treatment, but in ΔLhca4 the PSI antenna size was almost unchanged. These data suggest that in addition to the digitonin-insensitive PSI–LHCI–LHCII supercomplex, there is an 'extra' pool of LHCII trimers transferring energy to PSI in State II. Energy transfer from this extra LHCII to PSI is sensitive to the presence of digitonin and is largely absent in ΔLhca4. These results help explain earlier observations that LHCI could affect the energy transfer from LHCII to PSI in membrane preparations from spinach[36].

The increase in PSI antenna size occurring during state transitions is seen primarily in the grana margins (+37%), with a smaller increase observed for the stromal lamellae (+14%), consistent with the reports of Tikkanen *et al.*[17] and Kim *et al.*[37] The results showed the PSI antenna size in the grana margins was even larger than that seen in the isolated PSI–LHCI–LHCII supercomplex, supporting the notion that extra LHCII trimers are bound to PSI *in vivo*. Remarkably, our results demonstrate that even in the virtual absence of LHCII phosphorylation in State I, the PSI antenna size *in vivo* is still elevated compared with purified PSI–LHCI, due to interaction with trimeric LHCII. The $P700^+$ data allow us to estimate the absolute antenna size by assuming the purified PSI–LHCI complex corresponds to 155 chlorophylls[22,23]. Thus the PSI antenna size in the grana is ~180 chlorophylls (0.6 LHCII trimers/PSI) in State I and ~243 (2.09 trimers) in State II and in the stromal lamellae is ~166 (0.26 trimers) in State I and ~180 (0.6 trimers) in State II. Consistent with this suggestion, a detergent-free membrane preparation of PSI–LHCI binding up to five LHCII trimers was recently isolated from spinach using styrene-maleic acid copolymer[38]. Indeed, there are many previous reports in spinach and pea showing that PSI can be isolated with significant quantities of LHCII (refs 36,39–41) and that PSI in the grana margins has a larger antenna size due to binding of extra LHCII (refs 9,40,41).

It has been suggested that the large amount of LHCII trimers, which are recovered upon detergent solubilization of the *Arabidopsis* thylakoid membrane, unbound to either PSI or PSII, form an antenna

'lake' *in vivo* that can transfer energy to PSII and PSI (ref. 33). These extra LHCII trimers are found in both the grana and stromal lamellae regions of the membrane irrespective of the phosphorylation state of the thylakoid membrane and constitute as much as 45–66% of the LHCII trimer pool[33]. In our samples we measured an LHCII/ PSII ratio of 3.94, consistent with reported numbers[42]. Therefore two extra trimers per PSII exist in the membrane outside that found in the $C_2S_2M_2$ PSII–LHCII supercomplex. Our results support the proposal that these extra LHCII trimers can transfer energy to PSII and PSI *in vivo* with the balance dictated by the degree of phosphorylation[33]. They also indicate that in the absence of Lhca subunits that energy transfer from the LHCII 'lake' to PSI is perturbed, such that only the tightly bound LHCII within the PSI–LHCI–LHCII supercomplex is now efficiently transferring energy to PSI.

## Methods

**Plant growth.** Wild-type *Arabidopsis thaliana* (L.) ecotype Columbia (Col-0) plants and the T-DNA knockout light-harvesting complex I antenna mutants used in this study (ΔLhca1 (AT3G54890), ΔLhca2 (AT3G61470), ΔLhca3 (AT1G61520), ΔLhca4 (AT3G47470) were grown in a Conviron plant growth room with an 12 h photoperiod at a light intensity of 100 μmol photons $m^{-2}$ $s^{-1}$ and a day/night temperature 22/18 °C, respectively.

**PAM fluorescence.** Chlorophyll fluorescence was measured with a Dual PAM 100 chlorophyll fluorescence photosynthesis analyser (Walz). The fluorescence level with PSII reaction centres open (*Fo*) was measured in the presence of a 2 μmol photons $m^{-2}$ $s^{-1}$ measuring beam. The maximum fluorescence in the dark-adapted state (*Fm*) and during the course of actinic illumination (*Fm′*) was determined using a 0.8-s saturating light pulse (4,000 μmol photons $m^{-2}$ $s^{-1}$). Red light (30 μmols photons $m^{-2}$ $s^{-1}$) was provided by arrays of 635 nm LEDs illuminating both the adaxial and abaxial surfaces of the leaf. Far-red light was provided by 720 nm LEDs. State transitions fluorescence parameters (qS and qT) were calculated according to Ruban and Johnson[2].

**$P700^+$ absorption measurements.** P700 absorption was measured in the dual-wavelength mode (830–875 nm) of the Dual PAM 100. $P700^+$ formation kinetics were measured on isolated thylakoid membranes in the presence of 30 μM 3-(3,4-dichlorophenyl)-1,1-dimethylurea (DCMU), 100 μM methyl viologen and 500 μM sodium ascorbate (for measurement of purified PSI complexes DCMU was omitted and 0.01% *n*-dodecyl-α-d-maltoside added) to create a donor-limited situation. Under these conditions the rate of photo-oxidation of P700 is directly proportional to the PSI antenna size[43]. Traces were fitted with a single exponential functions and the tabulated data is the average of 4 traces per sample. The light intensity was 29 μmol photons $m^{-2}$ $s^{-1}$. PSI Antenna size calculated as (wild-type State I $t_{½}$ ÷ sample $t_{½}$) × 100% expressed as a percentage of wild-type State I antenna size with the assumption that all chlorophylls functionally connected to a reaction centre contribute equally to P700 oxidation[43].

**Isolation of thylakoid membranes in State I and State II.** Eight week old plants were given 1 h exposure to either PSII light provided by 660 nm LEDs (BML Horticulture) or PSI light provided by 730 nm LEDs (BML Horticulture). The light intensity of each treatment was 30 μmol photons $m^{-2}$ $s^{-1}$. Following light treatment thylakoids were prepared from the plants according to the method of Järvi *et al.*[31] with the addition that 10 mM NaF was included in all buffers. Grana and stromal lamellae were isolated from State I and State II thylakoids as described previously.[44]

**Protein purification.** PSI–LHCI and LHCII-PSI–LHCI were purified as described previously.[11] LHCII was purified as previously described.[45]

**SDS–PAGE.** State I and II thylakoids (5 μg of chlorophyll) were separated by SDS–PAGE.[45] Anti-phosphothreonine antibody (New England Biolabs) immunoblotting, Diamond Pro-Q Phospho staining (Life technologies) and SYPRO Ruby total protein (Life technologies) staining were performed as previously described.[17]

**Blue-native PAGE.** The supernatant from State I and II thylakoids solubilized by the digitonin method of Fristedt *et al.*[44] was subjected to BN–PAGE and subsequently separated by 2D-denaturing PAGE as described previously.[31]

**Low temperature fluorescence spectroscopy.** Chlorophyll (1 μM) from State I and State II thylakoids, grana, stromal lamellae or isolated complexes was suspended in the fluorescence buffer (60% glycerol, 300 mM sucrose, 5 mM $MgCl_2$, 20 mM HEPES pH 7.8) and measured in 1 cm polymethyl methacrylate cuvettes in a Opistat liquid nitrogen cooled bath cryostat (Oxford Instruments). Fluorescence emission and excitation measurements were performed as previously described[45] using a FluoroLog FL3–22 spectrofluorimeter (Jobin Yvon). The 735 nm excitation spectra were corrected for the PSII vibronic satellite contribution and normalized at 705 nm.[2] The 705 nm excitation spectra were normalized according to the change in the 685/735 nm emission ratio as described previously.[46] When assessing the effect of digitonin on thylakoid fluorescence (Fig. 4a), 0.5 mg/ml (chlorophyll) of thylakoids was solubilized with 1% digitonin for 20 min at room temperature and then diluted to 1 μM chlorophyll using fluorescence buffer supplemented with 0.06% digitonin and immediately frozen for measurement.

Received 11 May 2015; accepted 14 October 2015; published XX XX 2014

## References


1. Haldrup, A., Jensen, P. E., Lunde, C. & Scheller, H. V. Balance of power: a view of the mechanism of photosynthetic state transitions. *Trends in Plant Sci.* **6,** 301–305 (2001).
2. Ruban, A. V. & Johnson, M. P. Dynamics of higher plant photosystem cross-section associated with state transitions. *Photosynth. Res.* **99,** 173–183 (2009).
3. Horton, P. & Black, M. T. Activation of adenosine 5′-triphosphate induced quenching of chlorophyll fluorescence by reduced plastoquinone. The basis of State I–State II transitions in chloroplasts. *FEBS Lett.* **119,** 141–144 (1980).
4. Bellafiore, S., Barneche, F., Peltier, G. & Rochaix, J. D. State transitions and light adaptation require chloroplast thylakoid protein kinase STN7. *Nature* **433,** 892–895 (2005).
5. Pribil, M., Pesaresi, P., Hertle, A., Barbato, R. & Leister, D. Role of plastid protein phosphatase TAP38 in LHCII dephosphorylation and thylakoid electron flow. *PLoS Biol.* **8,** e1000288 (2010).
6. Shapiguzov, A., *et al.* The PPH1 phosphatase is specifically involved in LHCII dephosphorylation and state transitions in *Arabidopsis*. *Proc. Natl Acad. Sci. USA* **107,** 4782–4787 (2010).
7. Frenkel, M., Bellafiore, S., Rochaix, J. D. & Jansson, S. Hierarchy amongst photosynthetic acclimation responses for plant fitness. *Physiol. Plantarum* **129,** 455–459 (2007).
8. Tikkanen, M., Grieco, M., Kangasjärvi, S. & Aro, E. M. Thylakoid protein phosphorylation in higher plant chloroplasts optimizes electron transfer under fluctuating light. *Plant Physiol.* **152,** 723–735 (2010).
9. Albertsson, P. Å. A quantitative model of the domain structure of the photosynthetic membrane. *Trends Plant Sci.* **6,** 349–354 (2001).
10. Dekker, J. P. & Boekema, E. J. Supramolecular organization of thylakoid membrane proteins in green plants. *Biochim. Biophys. Acta* **1706,** 12–39 (2005).
11. Galka, P., *et al.* Functional analyses of the plant photosystem I-light-harvesting complex II supercomplex reveal that light-harvesting complex II loosely bound to photosystem II is a very efficient antenna for photosystem I in state II. *Plant Cell* **24,** 2963–2978 (2012).
12. Wientjes, E., Drop, B., Kouril, R., Boekema, E. J. & Croce, R. During state 1 to state 2 transition in *Arabidopsis thaliana*, the photosystem II supercomplex gets phosphorylated but does not disassemble. *J. Biol. Chem.* **288,** 32821–32826 (2013).
13. Kyle, D. J., Staehelin, L. A. & Arntzen, C. J. Lateral mobility of the light-harvesting complex in chloroplast membranes controls excitation energy distribution in higher plants. *Arch. Biochem. Biophys.* **222,** 527–541 (1983).
14. Chuartzman, S. G., *et al.* Thylakoid membrane remodeling during state transitions in *Arabidopsis*. *Plant Cell* **20,** 1029–1039 (2008).
15. Pietrzykowska, M., *et al.* The light-harvesting chlorophyll *a/b* binding proteins Lhcb1 and Lhcb2 play complementary roles during state transitions in *Arabidopsis*. *Plant Cell.* **26,** 3646–3660 (2014).
16. Bassi, R., Rigoni, F., Barbato, R. & Giacometti, G. M. Light-harvesting chlorophyll *a/b* proteins (LHCII) populations in phosphorylated membranes. *Biochim. Biophys. Acta* **936,** 29–38 (1988).
17. Tikkanen, M., *et al.* Phosphorylation-dependent regulation of excitation energy distribution between the two photosystems in higher plants. *Biochim. Biophys. Acta* **1777,** 425–432 (2008).
18. Lunde, C., Jensen, P. E., Haldrup, A., Knoetzel, J. & Scheller, H. V. The PSI-H subunit of photosystem I is essential for state transitions in plant photosynthesis. *Nature* **408,** 613–615 (2000).
19. Zhang, S. & Scheller, H. V. Light-harvesting complex II binds to several small subunits of photosystem I. *J. Biol. Chem.* **279,** 3180–3187 (2004).
20. Kouril, R., *et al.* Structural characterization of a complex of photosystem I and light-harvesting complex II of *Arabidopsis thaliana*. *Biochemistry* **44,** 10935–10940 (2005).
21. Boekema, E. J., *et al.* Green plant photosystem I binds light-harvesting complex I on one side of the complex. *Biochem.* **40,** 1029–1036 (2001).
22. Mazor, Y., Borovikova, A. & Nelson, N. The structure of plant photosystem I super-complex at 2.8 Å resolution. *eLife* **4,** e07433 (2015).
23. Qin, X., Suga, M., Kuang, T. & Shen, J.-R. Structural basis for energy transfer pathways in the plant PSI-LHCI supercomplex. *Science.* **348,** 989–995 (2015).
24. Klimmek, F. *et al.* Structure of the higher plant light harvesting complex I: *in vivo* characterization and structural interdependence of the Lhca proteins. *Biochemistry* **44,** 3065–3073 (2005).

25. Morosinotto, T., Ballotarri, M., Klimmek, F., Jansson, S. & Bassi, R. The association of the antenna system to photosystem I in higher plants. *J. Biol. Chem.* **280,** 31050–31058 (2005).
26. Wientjes, E., Oostergetel, G. T., Jansson, S., Boekema, E. J. & Croce, R. The role of Lhca complexes in the supramolecular organization of higher plant photosystem I. *J. Biol. Chem.* **284,** 7803–7810 (2009).
27. Zhang, H., Goodman, H. M. & Jansson, S. Antisense inhibition of the photosystem I antenna protein Lhca4 in *Arabidopsis thaliana*. *Plant Physiol.* **115,** 1525–1531 (1997).
28. Ganeteg, U., Strand, Å., Gustafsson, P. & Jansson, S. The properties of the chlorophyll *a*/*b*-binding proteins Lhca2 and Lhca3 studied *in vivo* using antisense inhibition. *Plant Physiol.* **127,** 150–158 (2001).
29. Ganeteg, U., Külheim, C., Andersson, J. & Jansson, S. Is each light-harvesting complex protein important for plant fitness? *Plant Physiol.* **134,** 502–509 (2004).
30. Ihalainen, J. A., *et al.* Excitation energy trapping in photosystem I complexes depleted in Lhca1 and Lhca4. *FEBS Lett.* **579,** 4787–4791 (2005).
31. Järvi, S., Suorsa, M., Paakkarinen, V. & Aro, E. M. Optimized native gel systems for separation of thylakoid protein complexes: novel super- and mega-complexes. *Biochem J.* **439,** 207–214 (2011).
32. Liu, Z. F., *et al.* Crystal structure of spinach major light-harvesting complex at 2.72 Å resolution. *Nature* **428,** 287–292 (2004).
33. Grieco, M., Suorsa, M., Jajoo, A., Tikkanen, M. & Aro, E. M. Light-harvesting II antenna trimers connect energetically the entire photosynthetic machinery — including both photosystems II and I. *Biochim. Biophys. Acta* **1847,** 607–619 (2015).
34. Jensen, P. E., Gilpin, M., Knoetzel, J. & Scheller, H. V. The PSI-K subunit of photosystem I is involved in the interaction between light-harvesting complex I and the photosystem I reaction center core. *J. Biol. Chem.* **275,** 24701–24708 (2000).
35. Varotto, C., *et al.* Single and double knockouts of the genes for photosystem I subunits G, K, and H of *Arabidopsis*. effects on photosystem I composition, photosynthetic electron flow, and state transitions. *Plant Physiol.* **129,** 616–624 (2002).
36. Bassi, R. & Simpson, D. Chlorophyll-protein complexes of barley photosystem I. *Eur. J. Biochem.* **163,** 221–230 (1987).
37. Kim, E., Ahn, T. K. & Kumazak, S. Changes in antenna sizes of photosystems during state transitions in granal and stroma-exposed thylakoid membrane of intact chloroplasts in *Arabidopsis* mesophyll protoplasts. *Plant Cell Physiol.* (2015). http://dx.doi.org/10.1093/pcp/pcv004.
38. Bell, A. J., Frankel, L. K. & Bricker, T. M. High yield non-detergent isolation of photosystem I-light harvesting chlorophyll II membranes from spinach thylakoids. *J. Biol. Chem.* **290,** 18429–18437 (2015).
39. Williams, R. S., Allen, J. F., Brain, A. P. R. & Ellis, R. J. Effect of $Mg^{2+}$ on excitation energy transfer between LHCII and LHCI in a chlorophyll-protein complex. *FEBS Lett.* **225,** 59–66 (1987).
40. Andreasson, E. & Albertsson, P. Å. Heterogeneity in Photosystem I - the larger antenna of Photosystem Iα is due to functional connection to a special pool of LHCII. *Biochim. Biophys. Acta* **1141,** 175–182 (1993).
41. Jansson, S., Stefansson, H., Nystrom, U., Gustafsson, P. & Albertsson, P. Å. Antenna protein composition of PS I and PS II in thylakoid sub-domains. *Biochim. Biophys. Acta* **1320,** 297–309 (1997).
42. Kouril, R., Wientjes, E., Bultema, J. B., Croce, R. & Boekema, E. J. High-light vs. low-light: Effect of light acclimation on photosystem II composition and organization in *Arabidopsis thaliana*. *Biochim. Biophys. Acta* **1827,** 411–419 (2013).
43. Melis, A. Kinetic analysis of P-700 photoconversion: effect of secondary electron donation and plastocyanin inhibition. *Arch. Biochem. Biophys.* **217,** 536–545 (1982).
44. Fristedt, R. *et al.* Phosphorylation of photosystem II controls functional macroscopic folding of photosynthetic membranes in *Arabidopsis*. *Plant Cell.* **21,** 3950–3964 (2009).
45. Ruban, A. V. *et al.* Plasticity in the composition of the light harvesting antenna of higher plants preserves structural integrity and biological function. *J. Biol. Chem.* **281,** 14981–14990 (2006).
46. Kiss, A., Crouchman, S., Ruban, A. V. & Horton, P. The PsbS protein controls the organisation of the photosystem II antenna in higher plant thylakoid membranes. *J. Biol. Chem.* **283,** 3972–3978 (2008).


## Acknowledgements

M.P.J. acknowledges funding from the Leverhulme Trust (U.K.) and the Krebs Institute and Project Sunshine at the University of Sheffield. A.V.R. gratefully acknowledges funding from the Biotechnology and Biological Sciences Research Council (U.K.), Leverhulme Trust and The Royal Society Wolfson Research Merit Award. C.N.H. and M.P.J. acknowledge research grant BB/M000265/1 from the Biotechnology and Biological Sciences Research Council (UK). C.N.H. was also supported by an Advanced Award 338895 from the European Research Council. This work was also supported as part of the Photosynthetic Antenna Research Center (PARC), an Energy Frontier Research Center funded by the US Department of Energy, Office of Science, and Office of Basic Energy Sciences under Award Number DE-SC0001035. PARC's role was to provide partial support for C.N.H.

## Author contributions

S.L.B., P.M., M.A.W. and M.J. performed experiments. M.P.J. analyzed the data. M.P.J, C.N.H., P.H., S.J. and A.V.R. designed the study and M.P.J. wrote the manuscript. All authors discussed the results and commented on the manuscript. P.H. and A.V.R. together carried out the preliminary experiments on which this study is based.

## Additional information

Supplementary information is available online. Reprints and permissions information is available online at www.nature.com/reprints. Correspondence and requests for materials should be addressed to M.P.J.

## Competing interests

The authors declare no competing financial interests.

Journal: NPLANTS

Article ID: nplants.2015.176

Article Title: An intact light harvesting complex I antenna system is required for complete state transitions in *Arabidopsis*

Author(s): Samuel L. Benson *et al.*

| Query Nos. | Queries | Response |
|---|---|---|
| Q1 | Please clarify what the qT method is | |
| Q2 | Please clarify what the 1-qP value stands for | |
| Q3 | Ref 37: please update the details if available | |
| Q4 | Figure 3b: please define the error bars | |